

2

TECHNICAL REPORT BRL-TR-3165

BRL

AD-A228 370

ROTATIONAL TEMPERATURE ESTIMATION OF CO
AT HIGH TEMPERATURES BY GRAPHICAL METHODS
USING FTIR SPECTROMETRY

KEVIN L. McNESBY
ROBERT A. FIFER

OCTOBER 1990

DTIC
ELECTE
NOV 01 1990
S B D

APPROVED FOR PUBLIC RELEASE; DISTRIBUTION UNLIMITED.

U.S. ARMY LABORATORY COMMAND

BALLISTIC RESEARCH LABORATORY
ABERDEEN PROVING GROUND, MARYLAND

NOTICES

Destroy this report when it is no longer needed. DO NOT return it to the originator.

Additional copies of this report may be obtained from the National Technical Information Service, U.S. Department of Commerce, 5285 Port Royal Road, Springfield, VA 22161.

The findings of this report are not to be construed as an official Department of the Army position, unless so designated by other authorized documents.

The use of trade names or manufacturers' names in this report does not constitute indorsement of any commercial product.

UNCLASSIFIED

REPORT DOCUMENTATION PAGE			Form Approved OMB No. 0704-0188	
<small>Public reporting burden for this collection of information is estimated to average 1 hour per response, including the time for reviewing instructions, searching existing data sources, gathering and maintaining the data needed, and completing and reviewing the collection of information. Send comments regarding this burden estimate or any other aspect of this collection of information, including suggestions for reducing this burden, to Washington Headquarters Services, Directorate for Information Operations and Reports, 1215 Jefferson Davis Highway, Suite 1204, Arlington, VA 22202-4302 and to the Office of Management and Budget, Paperwork Reduction Project (0704-0188), Washington, DC 20503</small>				
1. AGENCY USE ONLY (Leave blank)		2. REPORT DATE October 1990		3. REPORT TYPE AND DATES COVERED Final, Jun 88 - Dec 89
4. TITLE AND SUBTITLE ROTATIONAL TEMPERATURE ESTIMATION OF CO AT HIGH TEMPERATURES BY GRAPHICAL METHODS USING FTIR SPECTROMETRY			5. FUNDING NUMBERS 11161102AH43	
6. AUTHOR(S) Kevin L. McNesby Robert A. Fifer				
7. PERFORMING ORGANIZATION NAME(S) AND ADDRESS(ES)			8. PERFORMING ORGANIZATION REPORT NUMBER	
9. SPONSORING / MONITORING AGENCY NAME(S) AND ADDRESS(ES) Ballistic Research Laboratory ATTN: SLCBR-DD-T Aberdeen Proving Ground, MD 21005-5066			10. SPONSORING / MONITORING AGENCY REPORT NUMBER BRL-TR-3165	
11. SUPPLEMENTARY NOTES				
12a. DISTRIBUTION / AVAILABILITY STATEMENT Approved for public release; distribution unlimited			12b. DISTRIBUTION CODE	
13. ABSTRACT (Maximum 200 words) Rotational temperatures are obtained from gas phase Fourier transform infrared spectra of CO using graphical methods over the temperature range 302-773 K. Peak absorbances of individual ro-vibrational transitions are corrected for instrumental distortion and are then fit to a Boltzmann distribution to obtain the rotational temperature of the gas. A solution to the convolution integral for FTIR spectrometry is obtained by numerical integration. The equation relating observed peak observance, A_{obs} , to true peak absorbance, A_{pm} , ranging from one to five true peak absorbance units for triangularly apodized spectra is: $A_{pm} \propto A_{obs}^{1.818R^{1.748}}$ where R, the resolution parameter, is equal to $1/(2Da_n)$, a_n is the half width at half height (HWHH) of the absorption line in question, and D is the maximum optical retardation of the interferometer (here equal to 1 cm). In all cases, temperatures obtained by graphical analysis yielded gas temperatures within 10% of actual.				
14. SUBJECT TERMS Temperature Estimation, Infrared, Fourier Transformation			15. NUMBER OF PAGES 29	
			16. PRICE CODE	
17. SECURITY CLASSIFICATION OF REPORT Unclassified	18. SECURITY CLASSIFICATION OF THIS PAGE Unclassified	19. SECURITY CLASSIFICATION OF ABSTRACT Unclassified	20. LIMITATION OF ABSTRACT UL	

UNCLASSIFIED

INTENTIONALLY LEFT BLANK.

TABLE OF CONTENTS

	<u>Page</u>
LIST OF FIGURES.....	v
I. INTRODUCTION.....	1
II. BACKGROUND.....	1
III. CALCULATIONS.....	3
IV. EXPERIMENTAL.....	8
V. RESULTS AND DISCUSSION.....	10
VI. CONCLUSION.....	14
REFERENCES.....	17
DISTRIBUTION LIST.....	19



Accession For	
NTIS GRA&I	<input checked="" type="checkbox"/>
DTIC TAB	<input type="checkbox"/>
Unannounced	<input type="checkbox"/>
Justification	
By	
Distribution/	
Availability Codes	
Dist	Avail and/or Special
A-1	

INTENTIONALLY LEFT BLANK.

LIST OF FIGURES

<u>Figure</u>		<u>Page</u>
1	A Portion of the IR Spectrum of CO at 866 K.....	5
2	Line Center Separation Between the $v=0-1$ and $v=1-2$ Transitions in CO.....	6
3	Line Center Separation Between the $v=0-1$ Transition in ^{12}CO and the $v=0-1$ Transition in ^{13}CO	7
4	Experimental Setup for Burner Flame Experiments.....	9
5	A Plot of $-E(m)/k$ vs. $-\ln(A_{\text{obs}}^x / ((2Da_{m,0})^{y-1} m F(m) v_m))$ for Samples of CO Held in the Temperature Controlled Cells Over the Temperature Range 302 K to 773 K.....	12
6	Spectrum of a Rich $\text{CH}_4/\text{N}_2\text{O}$ Flame at 64 Torr.....	13
7	A Plot of $-E(m)/k$ vs. $-\ln(A_{\text{obs}}^x / ((2Da_{m,0})^{y-1} m F(m) v_m))$ for CO $v=1-2$ P Branch Transitions in a Low Pressure (64 Torr) $\text{CH}_4/\text{N}_2\text{O}$ Flame.....	15

INTENTIONALLY LEFT BLANK.

I. INTRODUCTION

The theory and technique for determining the temperatures of gases from their Fourier transform infrared spectra, in emission and absorption, has been well documented in the literature.¹ Frequently, temperature determination involves fitting peak absorbances of rotational fine structure within a vibrational transition to a Boltzmann-type population expression,² since the relative absorbances are strongly temperature dependent. One of the difficulties associated with calculating the temperature of a gas from the peak absorbances of ro-vibrational transitions is instrumental distortion of peak absorbance values. This distortion results from the convolution of the source intensity (modulated by the sample) and the instrument lineshape function (ILS), and is most important in spectra obtained at moderate to low resolution (here taken to correspond to optical retardations of less than ~ 1.0 cm). The method for correcting the error in observed peak absorbance due to this convolution as applied to FTIR spectroscopy was first described by Griffiths.³

The analytical treatment of most physically encountered convolutions is difficult.⁴ To our knowledge, no analytical solution to the resulting "convolution integral" for transmission spectra obtained on a FTIR spectrometer has been reported. We have recently investigated and quantified the relationship between observed and undistorted peak absorbances measured by FTIR spectroscopy. This relationship was first quantified by Griffiths and Anderson.³ Our goal is to develop a reasonably accurate (within $\sim 5\%$) graphical method to obtain the temperature of a gas sample at elevated temperatures (> 500 K) from absorption spectra in the infrared using resources typically available in an analytical laboratory. We assume this to be a Fourier transform IR spectrometer capable of 1 cm^{-1} resolution and a microcomputer of virtually any type. The graphical method is not intended to supplant the more accurate methods already in the literature,^{1,5} but rather to provide a fast and convenient complementary view of the data. To date, we are unaware of any successful temperature estimations from peak absorbances of ro-vibrational transitions which have employed graphical methods over a temperature range of several hundred degrees.

II. BACKGROUND

For a Fourier transform spectrometer employing triangular apodization of the interferogram, the observed minimum transmittance, T_m , of an absorption feature with a Lorentzian profile centered at frequency ν_m , may be given by:⁵

$$T_m = \int_{-\infty}^{\infty} \exp\{-2.303 A_{pm} a_m^2 / ((\nu - \nu_m)^2 + a_m^2)\} D \sin^2[\pi D(\nu - \nu_m)] / [\pi D(\nu - \nu_m)]^2 d\nu \quad (1)$$

where A_{pm} is the true peak absorbance of line p at frequency ν_m , a_m is the linewidth, D is the maximum optical retardation of the spectrometer, and π is 3.1416. Here, m is the line index number, where $m = -J''$ for P branch transitions and $m = J'' + 1$ for R branch transitions.⁶ This equation describes the minimum transmittance of an isolated pressure broadened line where the absorption feature is unobscured by any neighboring lines. Equation (1) is a function of temperature through the dependence of the linewidth, a_m , on

temperature. The variation of a_m with temperature and pressure may be calculated by the approximation:

$$a_m(T,P) = a_{m0}(P/P_0) (T_0/T)^n \quad (2)$$

where P_0 and T_0 are a pressure and temperature for which the linewidth a_{m0} is known, P and T are the experimental pressure and temperature, and n is the empirically determined temperature broadening exponent. The coefficient n has been shown⁸ to be temperature and line dependent. For the sake of simplification, n is usually set to 0.75, although there is evidence⁸ that a value of 0.66 may be more accurate at room temperature.

True peak absorbance may be fit to temperature, T , using:⁹

$$A_{pm} \propto |m| F(m) v_m \exp\{-E(m)/kT\} / a_m \quad (3)$$

where a_m varies as in Eq. (2), $E(m)$ is the rotational energy of the lower state in the transition, $F(m)$ is the Hermann-Wallis factor for interaction of rotation and vibration,⁶ and $|m|$ is the absolute value of the line index number. The linewidth appears in the denominator of Eq. (3) to take into account the dependence of the peak height on peak width for a spectral absorption feature with a Lorentzian profile.¹⁰

By substituting Eq. (2) into Eq. (1) and obtaining an analytical solution to the integral, an expression relating observed minimum transmittance (and hence observed peak absorbance) to true peak absorbance may be obtained. If we denote this expression as:

$$A_{pm} = f(T_m, a_m, D) \quad (4)$$

and combine this with Eq. (3) we obtain:

$$f(T_m, a_m, D) \propto |m| F(m) v_m \exp\{-E(m)/kT\} / a_m \quad (5)$$

The first step in linearizing Eq. (5) involves finding an approximation to Eq. (1). Griffiths gives the expression:^{3,5}

$$A_{pm} \propto A_{obs} x^R y \quad (6)$$

where R , the resolution parameter, is equal to $1/(2Da_m)$ and x and y are set equal to 2. If this expression is substituted into Eq. (5), and the temperature broadening exponent n is assumed to be invariant with m , one obtains:

$$A_{obs}^x / \{(2Da_{m0})^{y-1} (|m| F(m) v_m)\} \propto \exp\{-E(m)/kT\} \quad (7)$$

When ambient temperature spectra are collected (for which the a_m for many diatomics are accurately known)¹¹ and the resolution parameter for the ro-vibrational lines being used in the calculation is such that there is a near linear relationship³ between $\log(A_{pm})$ and $\log(A_{obs})$, a graph of $E(m)/k$ vs. $\ln[A_{obs}^x / \{(2Da_{m0})^{y-1} (|m| F(m) v_m)\}]$ produces a straight line with a slope $(1/T)$ the inverse of which usually falls within a percent of the true gas temperature.⁹ As the temperature of the gas being investigated is increased, the error between the calculated and actual temperature increases.⁵ This

increase in error is caused by the change in a_m with T , which affects the resolution parameter R , and may shift the relationship between $\log(A_{pm})$ and $\log(A_{obs})$ into a nonlinear region. Also, as stated earlier, the temperature broadening exponent, n , from Eq. (2) changes with temperature and, for a given temperature, may vary with line index number.

III. CALCULATIONS

We have fit input parameters and the result of the numerical integration of Eq. (1) to an equation of the form:

$$A_{pm} = k A_{obs}^{xR^y} \quad (8)$$

where k , x , and y are constants and R is the spectral resolution parameter. The integral in Eq. (1) was evaluated numerically for all combinations of optical retardations of 1, 2, 4, 8, and 10 cm, true peak absorbances of 0.1 to 10 (in intervals of 0.1) with absorbing lines for which a_m ranged from 0.01 to 0.1 cm^{-1} (in intervals of 0.01 cm^{-1}). A weighted line - least squares routine was used to fit the data from portions of the numerical integration of Eq. (1) to a linearized form of Eq. (8).

The integration routine assumed that ν_m was located at 2000 cm^{-1} , and elevated Eq. (1) using Simpson's $1/3$ rule for 50 cm^{-1} on either side of ν_m . The interval to be numerically integrated was divided into 10,000 segments. The choice of value for the center of absorption, ν_m , is arbitrary, as may be verified by substituting $\nu - \nu_m$ in Eq. (1). To determine if numerical integration gave values dependent on the value of ν_m ranging from 500 to 3500 cm^{-1} showed the value of the integral to be independent of the value for this parameter.

The application of our numerical integration routine to the function $\sin^2 x/x^2$ (which is similar in behavior to Eq. (1) yet has an analytical solution) using parameters similar to those in the numerical integration of (1) gave results within 0.001% of the analytical solution. We believe our numerical integration of Eq. (1) gives similar accuracy.

For all ranges of A_{pm} , values used in the integration of Eq. (1), the average deviation between the numerically integrated value $-\log(T_m)$ and the fitted approximation presented here was less than that of Eq. (6) with x and y equal to 2. In fairness, the authors of Reference 5 presented their approximation without derivation and in no way implied it to be valid over any range other than that specified in the paper. In addition, for the range over which the approximation of Reference 5 was used, that approximation and the fitted approximation developed here are in good agreement.

For spectra of gases below 800 K, the integral in Eq. (1) was evaluated for true peak absorbances, A_{pm} , ranging from 1 to 5 absorbance units, an optical retardation of 1 cm, and a_m values ranging from 0.01 to 0.1 cm^{-1} . These parameters are typical for CO at pressures of several hundred torr.⁵ The best fit values obtained for $\ln(k)$, x , and y in Eq. (8) were 0.122 (.014), 1.818 (.014), and 1.748 (.015), respectively, where the numbers in parentheses are equal to one standard deviation. For the same parameters mentioned above, but for peak absorbances ranging from 0.1 to 1.0 absorbance units, the best fit values of $\ln(k)$, x , and y were respectively, 0.211 (.00004), 1.287

(.00002), and 1.298 (.00002). The spectroscopic constants used to calculate $E(m)$ and $F(m)$ may be found in Reference 13. Values of v_m used in the calculation are those reported by the spectrometer. Values of a_m were obtained from Reference 5. For this work, it was assumed that all gases had the same broadening effect on the a_m for CO as did CO. The additional error¹¹ probably is insignificant given the assumption that n is constant.

At temperatures below 600 K, 20 lines from the R branch (because it is more intense than the P branch and for reasons given below) in the fundamental absorption band of CO were used in the calculation. To calculate the temperature, Eq. (7) was first linearized, and a weighted linear least squares¹⁴ routine used to determine $1/T$.

To decide which lines will be used to calculate temperatures from FTIR spectra, it is necessary to establish a criteria for line acceptability. Lines which are significantly overlapped by absorbances due to hot band transitions or to absorbances by isotopically substituted homologues should be excluded from the computation. Figure 1 shows a portion of the CO spectrum in a cell held at 866 K. Visible in this figure are absorbances due to ^{13}CO and those due to the 1-2 transition in ^{12}CO , as well as the much more intense fundamental transition. The error caused by hot band overlap is very temperature sensitive and becomes most important at high temperature. Figures 2 and 3 show the line center separation in wavenumbers between fundamental and hot ($v=1-2$) band transitions in ordinary CO between fundamental transitions in normal and ^{13}C substituted CO, respectively. These figures were generated by calculating rotational energy levels from spectroscopic constants¹³ for the appropriate species/vibrational level, calculating transition frequencies using conventional selection rules,¹⁵ ordering these transitions with respect to the energy of transition, and then taking the difference in energy between each successive level. This energy difference is plotted versus the energy of the transition with the lower energy. For each species considered, J'' values from 0 or 1 to 30 were used. At a glance, each of these figures provides a good idea of where regions of minimum line overlap exist for the fundamental absorption of CO. Because these figures do not include intensities of individual transitions, they cannot indicate where a weak fundamental absorption line used in the calculation is overlapped by a significantly strong ^{13}CO line, for example, or vice versa. For CO, typical ranges of lines to use in the calculation are the 20 lines in the regions $2059-2139\text{ cm}^{-1}$ (P-branch $J''=1-20$) and/or $2147-2212\text{ cm}^{-1}$ (R-branch $J''=0-19$). An examination of Figure 2 shows that these two regions of the fundamental absorption in CO significantly overlap with the $v=1-2$ transitions in CO, with the P branch being slightly less obscured. However, since the 1-2 envelope is shifted by about 25 cm^{-1} to lower energy than the 0-1 envelope (not apparent from the figure), the R branch of the 0-1 transition is relatively unobscured by those 1-2 transitions which have appreciable intensity at normal temperatures.

Figure 3 shows that both branches in the fundamental absorption of ^{12}CO have several lines with separation between line centers for overlap with ^{13}CO of less than 0.5 cm^{-1} . However, because the band centers differ between CO and ^{13}CO by about 45 cm^{-1} , the R branch of CO is relatively unobscured by overlap from the R branch of ^{13}CO (since the R branch of ^{13}CO overlaps the P branch of CO). Therefore, Figures 2 and 3 suggest using the R-branch of CO for temperature determinations at temperatures where hot band transitions are not important. At higher temperatures, Figure 3 suggests a switch to the

CO at 593 C using .125 cm-1 resolution

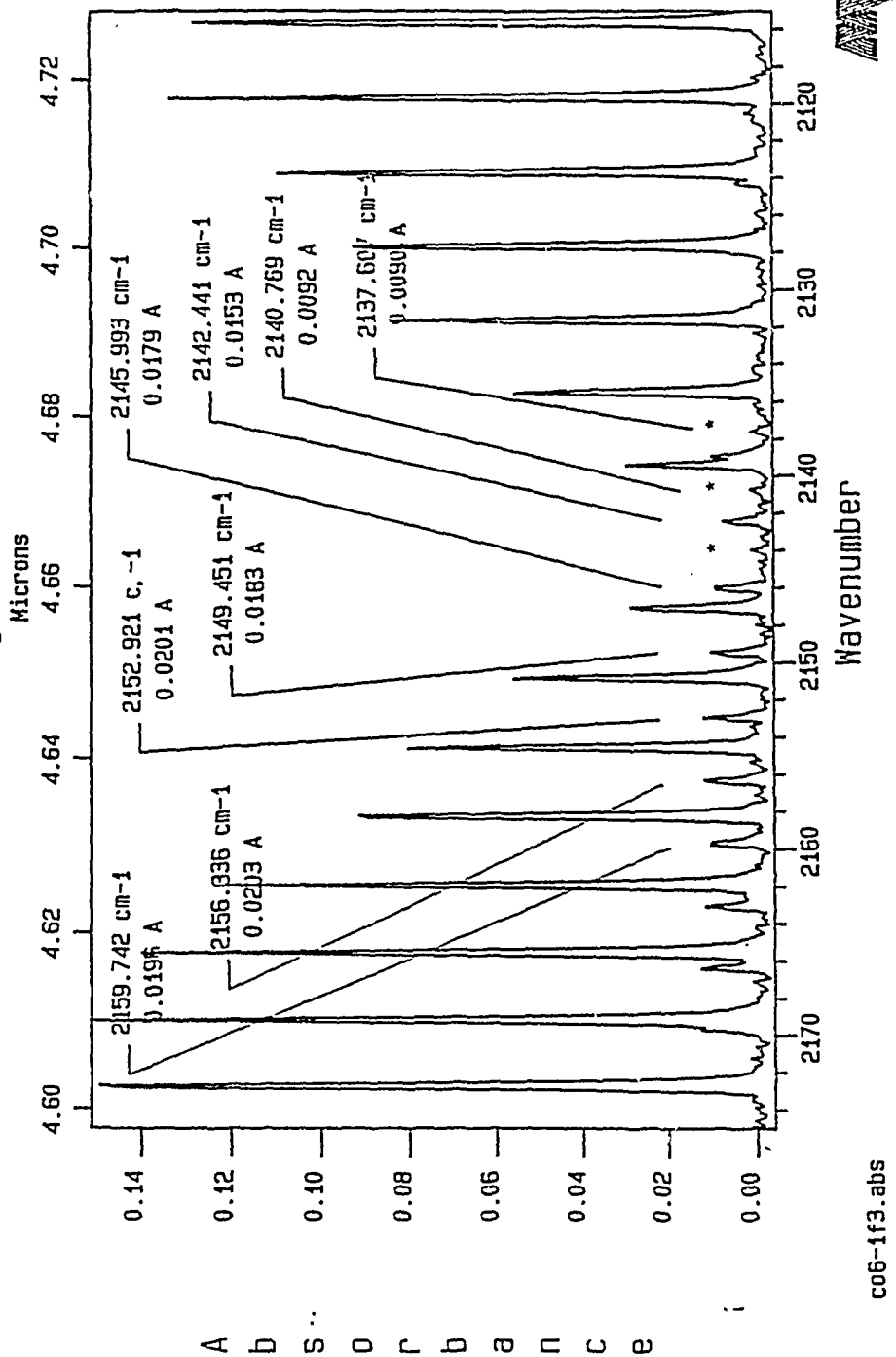


Figure 1. A portion of the IR Spectrum of CO at 866 K. Absorbances marked * are due to ¹³CO; otherwise, annotated peaks are due to the v=1-2 transition in CO. The most intense peaks are due to the fundamental absorption in CO.

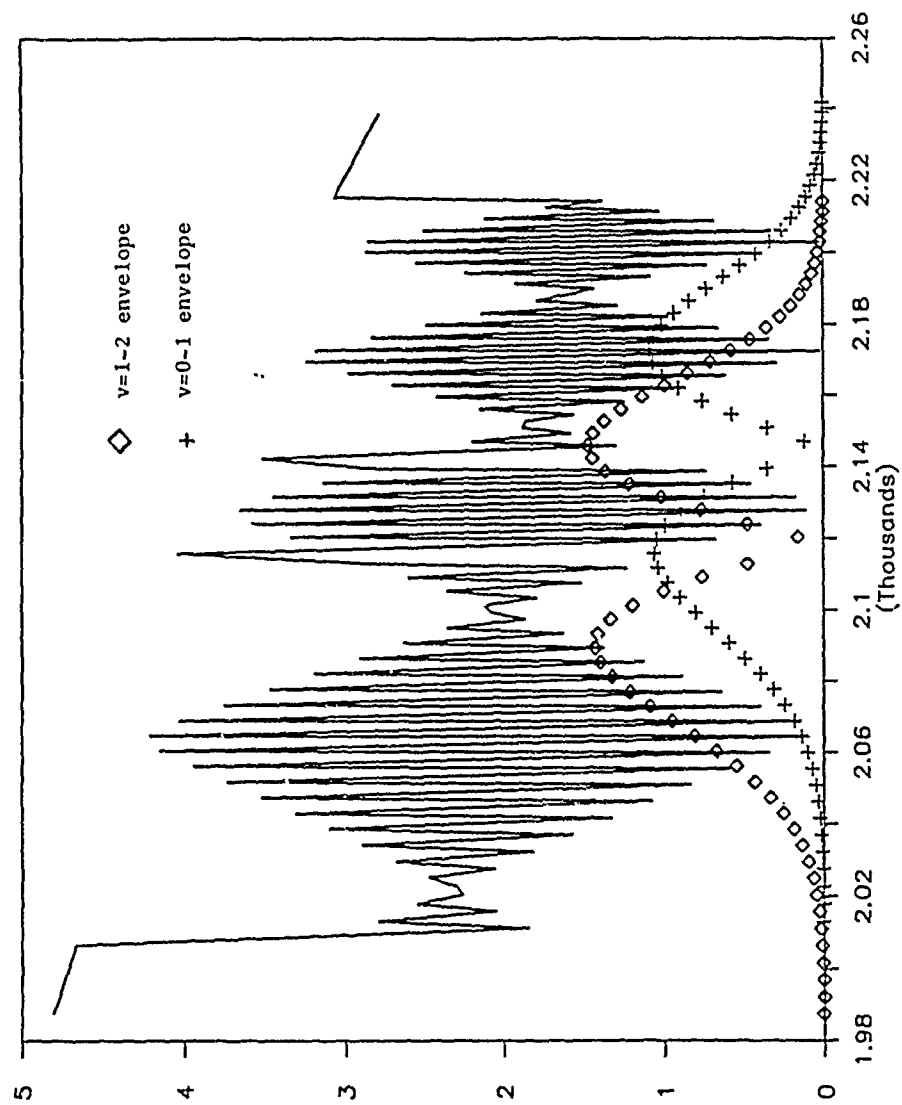


Figure 2. Line Center Separation Between the $v=0-1$ and $v=1-2$ Transitions in CO (see text)

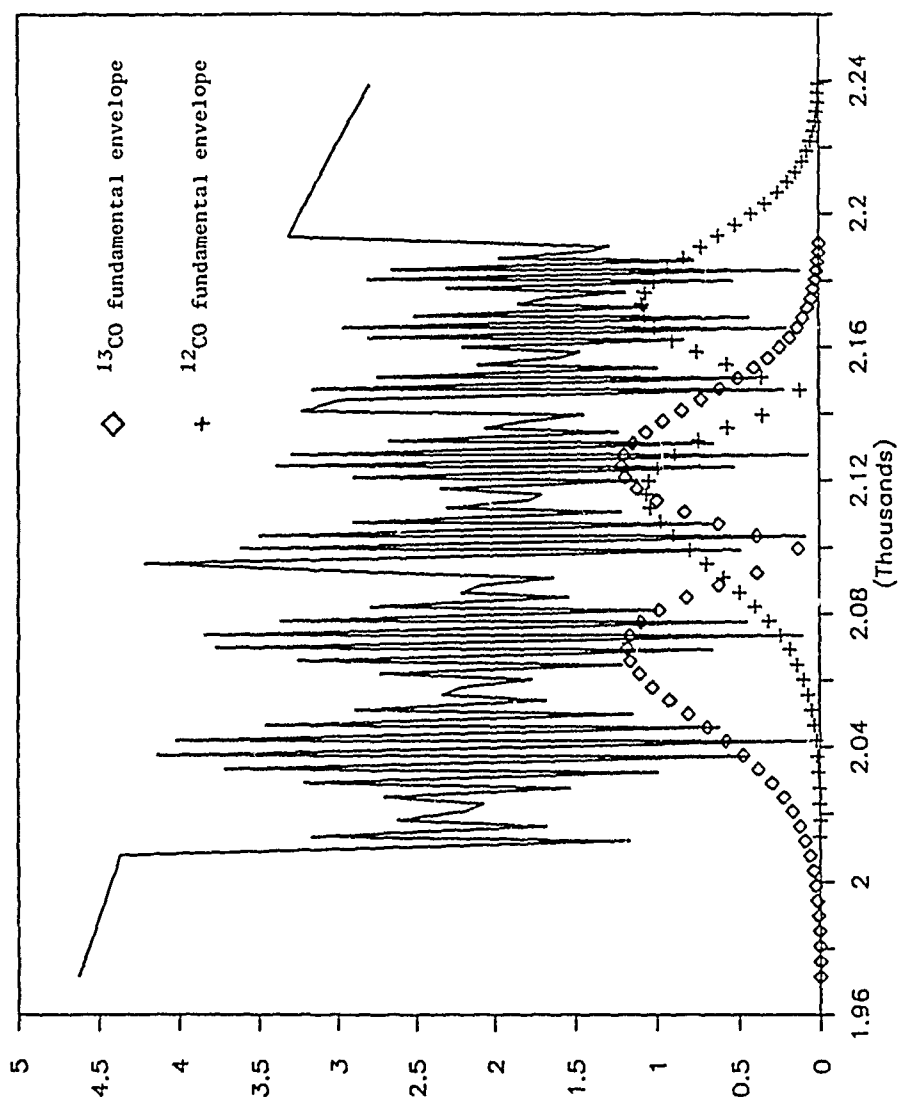


Figure 3. Line Center Separation Between the $v=0-1$ Transition in ^{12}CO and the $v=0-1$ Transition in ^{13}CO (see text)

P-branch of CO for temperature determinations when 1-2 transitions become more troublesome than ^{13}CO transitions.

IV. EXPERIMENTAL

All temperatures reported here were obtained from absorption spectra. Since the heated cell/burner was located in the sample compartment of an otherwise unmodified FTIR, infrared emission was unmodulated, and no attempt was made to collect emission spectra. No correction was made to the spectra to account for emission. Experiments were performed on a Mattson Sirius 100 FTIR spectrometer using a HgCdTe liquid nitrogen cooled detector. All spectra were obtained with 100 co-added scans obtained at 1 cm^{-1} resolution. Interferograms were triangularly apodized and zero-filled to the limit of our computer memory (131072 points) prior to transformation.

Temperature controlled stainless steel cells were equipped with NaCl windows. The pathlength for absorption in each cell was approximately 12 cm. For the temperature range 300 K to 473 K, the NaCl windows were attached to the cell body using metal flanges and fiber gaskets. The leak rate of this cell at all temperatures used was always less than 500 mtorr/hr. Pressures used in these low temperature experiments ($<473\text{ K}$) ranged from 115 to 197 torr. For the temperature range from 473 K to 773 K the NaCl windows were attached directly to the cell body by pressure supplied by flanges. To prevent heat loss, the high temperature cell was encased in asbestos which extended approximately 1 inch past the windows on either side of the cell. No other precautions were taken to avoid temperature gradients along the optical pathlength. The leak rate of this cell was such that all high temperature experiments were performed at 760 torr total pressure using a 4:1 mixture of air:CO. A check of the instrument after filling this cell, allowing it to stand for a typical time of one experiment (~ 10 minutes) and then evacuating the cell gave no CO absorption due to CO in the optical compartment of the spectrometer.

Temperature was controlled by an Omega Model 2010 temperature controller using heating cartridges placed in cavities in the cell body and monitored by copper-constantin thermocouples placed near the inner wall of the cell and placed within the gas volume but out of the optical path. A check of the cell temperature by an Omega Model 2168A digital thermometer inserted into the body of the cell gave temperature readings within 5 K of those reported by the controller thermocouple. All temperatures reported as actual are the temperatures of the cell body. After filling the cell, the gas was allowed to stand for three to five minutes to reach the temperature of the cell. Waiting for longer periods of time gave no significant change in calculated temperature. No correction was made for temperature variations in the vicinity of the cell windows. At temperatures greater than 550 K, some conversion of CO to CO_2 was observed for the cell containing CO plus air.

The experimental setup for the low pressure flame experiments is shown in Figure 4. The optical pathlength within the burner chamber was approximately 6 cm. The burner head was constructed entirely of Pyrex, with the burner housing constructed of brass and aluminum. Gas flow to the mixing section below the burner head was regulated by calibrated floating-ball type flowmeters. Pressure was measured using an MKS Instruments Baratron capacitance manometer and regulated by adjusting a valve downstream from the

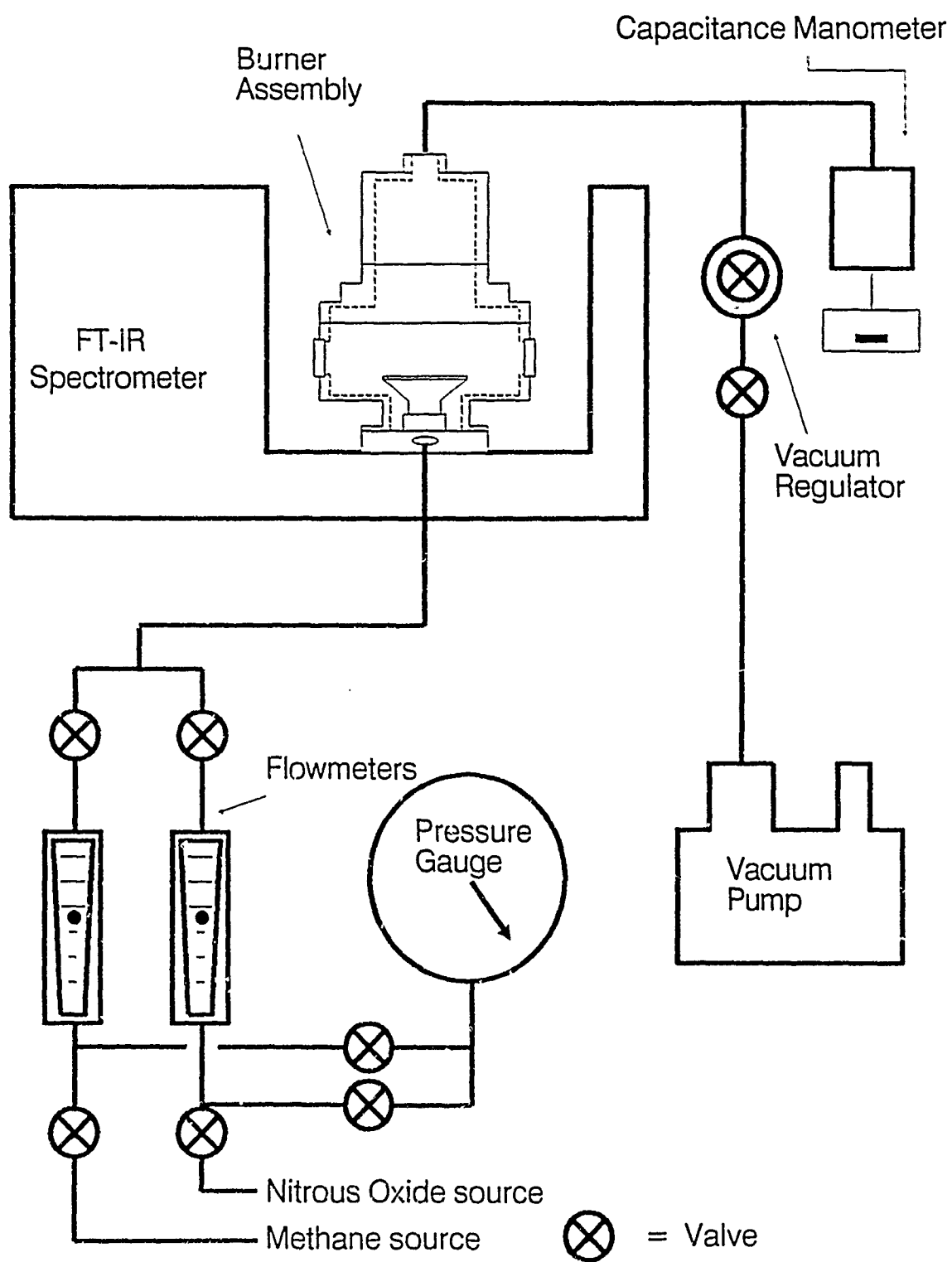


Figure 4. Experimental Setup for Burner Flame Experiments

flowmeters. Windows were of LiF. A low pressure (<100 torr operation), the flame is lifted off the burner surface by 2-4 mm, preventing damage to the Pyrex burner frit. Data was collected at the maximum iris setting of the spectrometer. Although maximizing sample compartment aperture increases the likelihood of resolution errors due to beam divergence, the beam waist at all times was kept within the limits built into the spectrometer. No correction was applied to reflect any non-collimated beam related errors.

V. RESULTS AND DISCUSSION

The results of temperature calculations using the temperature controlled gas cells for the range 300 K to 773 K are shown in Table 1. Values of x and y used in calculations over this temperature range were 1.818 and 1.748, respectively. At temperatures above 600 K, the P branch of the ro-vibrational envelope of CO was used in the calculations (see discussion above). Figure 5 shows a plot of $E(n)/k$ vs. $\ln(A_{\text{obs}}^x / \{(2Da_{m,0})^{y-1} |n| F(n) v_m\})$ for samples of CO held in the temperature controlled cells over the temperature range 302 K to 773 K. The slope of the best straight line through each set of data obtained by the weighted linear least squares routine¹⁴ is equal to $1/T$. In all cases, calculations yield gas temperatures within 10% of the cell temperature. Neglecting the one calculated point at 620 K, calculated temperatures are within 5% below 700 K. The best results were obtained when the temperature of the gas was near 400 K. This is in contrast to earlier work⁵ in which the best results were found at room temperature. The reason for this difference is that our fit to Eq. (1) is more accurate for small values of A_{pm} (<3) than for cases where x and y in Eq. (6) are equal to 2. As average peak absorbances of individual lines decrease with increasing temperature (total number of lines increases), an approximation to Eq. (1) which emphasizes small values of A_{pm} yields a temperature that is closer to actual than when x and y in Eq. (6) are equal to 2.

The curvature in the far right-hand side of the plots in Figure 5 in the region corresponding to low values of J'' is analogous to that seen in Reference 5. This arises from the fact that CO fundamental absorbances with low values of J'' have the largest a_m and smallest value of the resolution parameter, R . Spectra of lines with small resolution parameters and small absorbances have been shown^{3,5} not to adhere to a linear relationship between $\log(A_{\text{pm}})$ and $\log(A_{\text{obs}})$ when obtained using triangular or sinc² instrument line shape (ILS) functions.

Figure 6 shows a portion of the absorbance spectrum of a rich low pressure (64 torr) premixed methane/nitrous oxide burner flame used in the calculation of rotational temperatures of CO. The CO hot band ($v=1-2$) P branch transitions were chosen for the analysis because the hot band transitions are shifted to lower energy than those transitions of the fundamental. Also, interference from CO₂ bands around 2349 cm⁻¹ and from N₂O bands around 2223 cm⁻¹ makes finding suitable lines in the fundamental of CO difficult. Hot band transitions were chosen to discriminate against any cold CO near the inner surfaces of the burner chamber windows. Peaks were identified by calculating the peak locations for the $v=1-2$ ro-vibrational envelope of CO from spectroscopic constants.¹³ All calculations agreed within a few hundredths of a wavenumber with the peak locations reported by the

Mattson peak picking software. Table ^ shows calculated CO rotational temperatures as a function of the distance of the center of the IR beam above the burner frit surface.

Table 1. Calculated and Actual CO Temperatures for the Temperature Controlled Gas Cells Used in These Experiments Over the Range 302 to 773 K

<u>Actual Temperature (Kelvin)</u>	<u>Calculated Temperature (Kelvin)</u>	<u>Standard Deviation (Kelvin)</u>	<u>Total Pressure (torr)</u>	<u>Actual-Observed Temperature (Kelvin)</u>
302	299	4	166.8	3
302	297	4	164.7	5
302	296	4	166.8	6
313	306	5	760	7
322	313	3	196.7	9
323	319	5	163	4
325	323	6	141.8	2
332	324	4	184.7	8
343	335	4	195.1	8
343	337	4	189.6	6
344	340	6	152.1	4
363	364	7	127.3	-1
364	360	5	190.3	4
364	360	4	193.5	4
373	369	5	194	4
373	369	5	196.2	4
374	373	6	164	1
413	415	9	140.9	-2
413	416	9	141.4	-3
432	432	8	164.8	0
433	436	11	115.1	-3
438	437	8	184.6	1
473	477	3	760	-4
473	478	5	760	-5
576	602	9	760	-26
592	594	16	760	-2
674	620	61	760	54
674	672	13	760	2
674	673	40	760	1
773	758	23	760	15
773	813	48	760	-40
773	817	35	760	-44

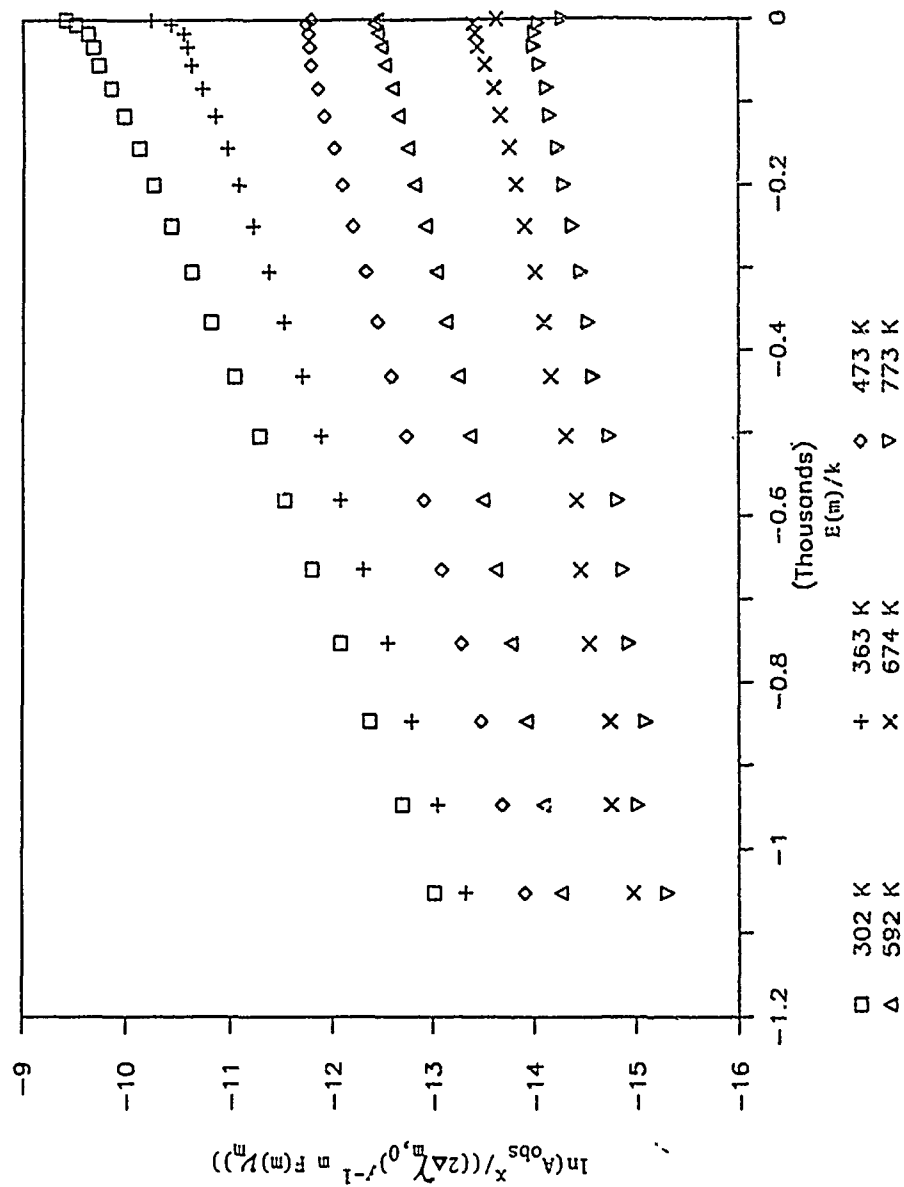


Figure 5. A Plot of $-\ln(A_{\text{obs}}^x / ((2\Delta\chi_{m,0})^{x-1} F(m) V_m^x))$ for Samples of CO Held in the Temperature Controlled Cells Over the Temperature Range 302 K to 773 K. The slope of each line is equal to T^{-1} . The abscissa for each set of data has been shifted to eliminate overlap of data sets.

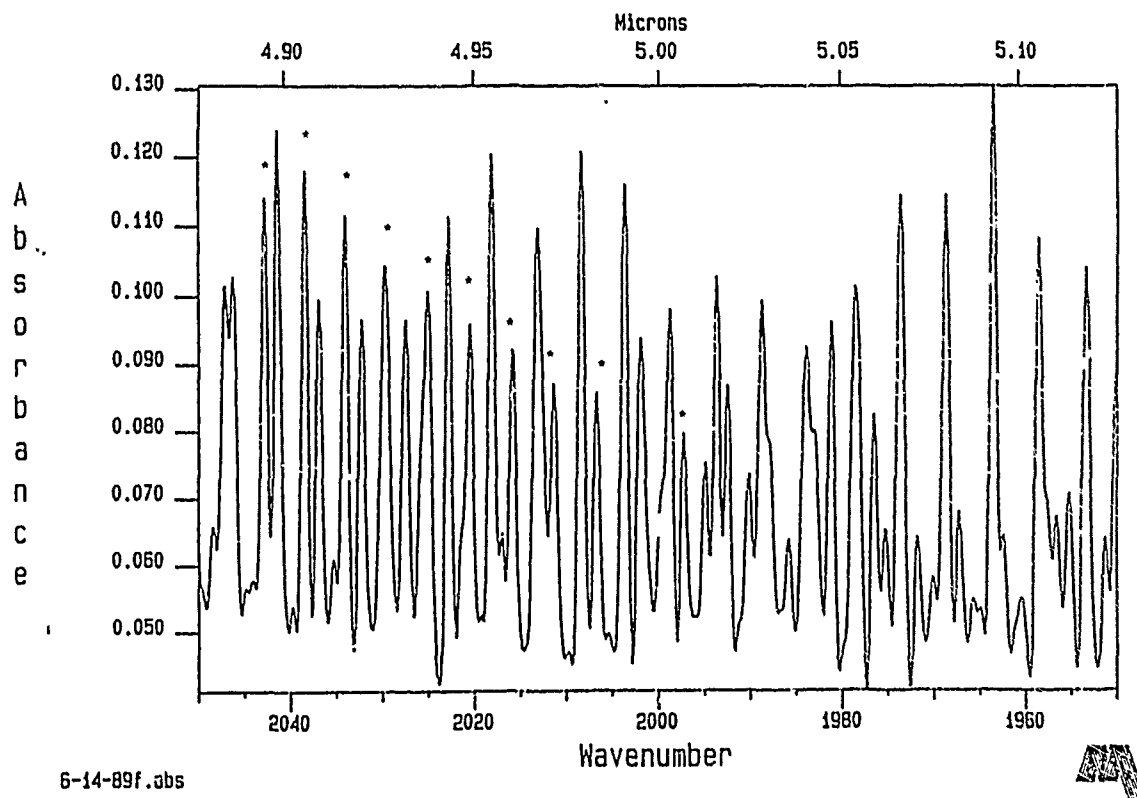


Figure 6. Spectrum of a Rich $\text{CH}_4/\text{N}_2\text{O}$ Flame at 64 Torr. Peaks marked with * are due to the P branch of the $v=1-2$ transition in CO.

Table 2. Calculated CO Rotational Temperatures as a Function of the Distance Between the Center of the IR Beam and the Burner Frit Surface

Burner Surface to Beam Center (cm)	Observed Temperature (Kelvin)	Standard Deviation (Kelvin)
0.5	1524	107
0.9	1516	107
1.3	1517	106
1.7	1515	113
2.1	1518	111
2.5	1542	111
2.9	1559	105
3.3	1579	107
3.7	1639	105
4.1	1704	110

Figure 7 shows a plot of $E(m)/k$ vs. $\ln(A_{\text{obs}}^x / \{(2Da_{m,0})^{y-1} |m| F(m) v_m\})$ for the burner flame experiments. Since the observed absorbances are very weak (maximum less than 0.12), we used the approximation to true peak absorbance from observed peak absorbance for the range of true peak absorbance from 0.1 to 1.0 ($x=1.287$, $y=1.208$). The flame temperatures reported here are lower than adiabatic for the methane/nitrous oxide flame system.¹⁶ We believe this is because the small burner chamber acted as a heat sink for the flame. No thermocouple measurements were made of the flame temperature within the burner chamber. Also, because we were unable to find published data for the a_m of the hot band spectral, we used the values for the fundamental. Finally, we made no provision for broadening of the CO lines by gases other than CO, so in effect, we were treating our data as if it were obtained in a chamber of pure CO. Our reasons for this stemmed from the many different species present in the flame and our inability at this time to quantify many of these species, particularly nitrogen.

VI. CONCLUSION

Calculations of rotational temperatures of CO at high temperatures and of CO participating in combustion reactions by use of simple graphical methods applied to FTIR spectra have been shown to be accurate within 10% (and usually much less) of actual temperature up to 800 K. Graphical analysis of the ro-vibrational structure of the fundamental absorption of CO gives results which indicate that the simple method employed here has practical applications, especially when an accurate approximation to true peak absorbances is used. Results from spectra of flames are encouraging but more work is needed. We are presently engaged in pursuing this area of research.

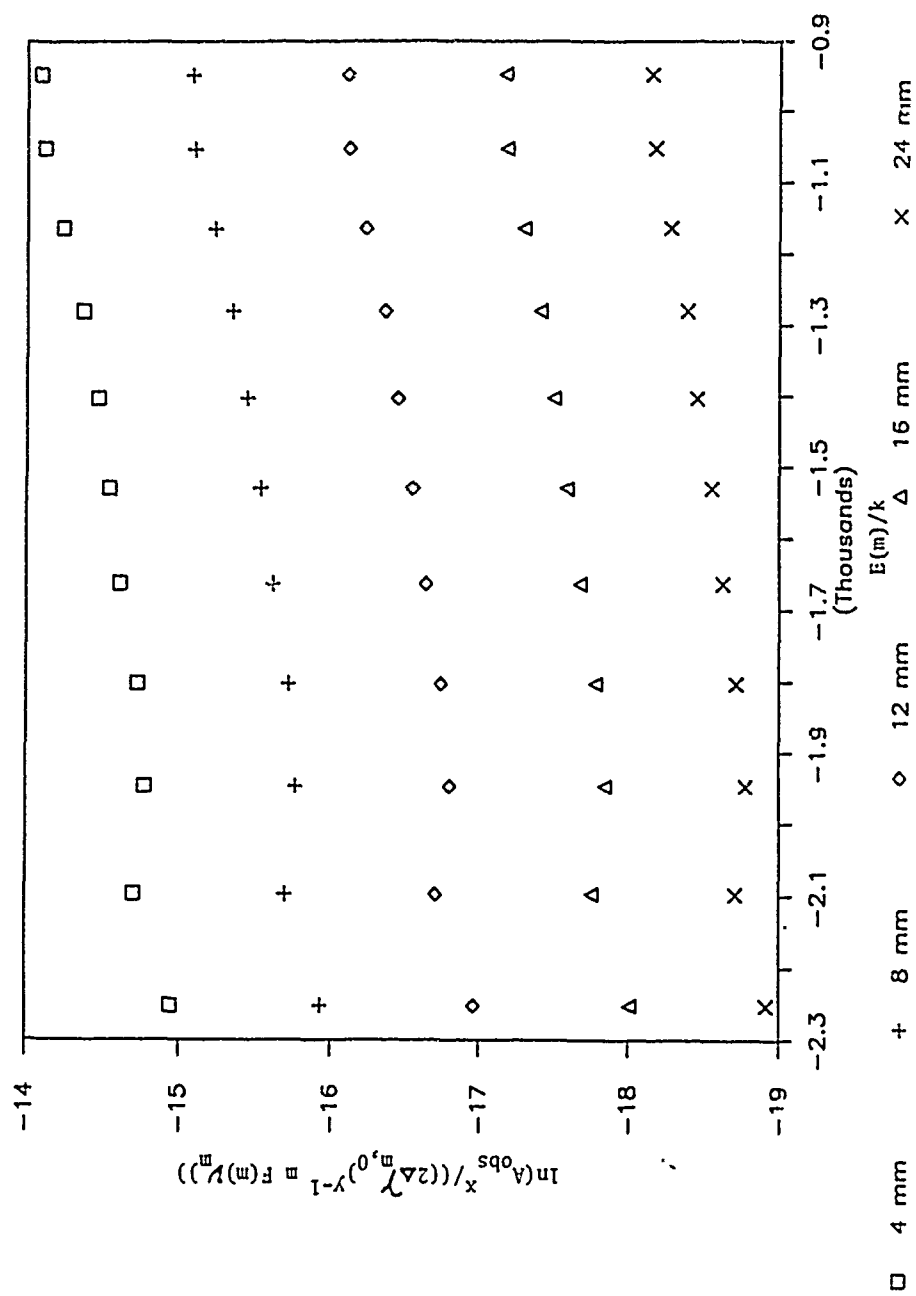


Figure 7. A Plot of $-\ln(A_{\text{obs}}^x / ((2\Delta_{m,0})^{y-1} |F(m)v_n|))$ for CO v=1-2 P Branch Transitions in a Low Pressure (64 torr) $\text{CH}_4/\text{N}_2\text{O}$ Flame. The abscissa for each set of data has been shifted to eliminate overlap of data sets.

INTENTIONALLY LEFT BLANK.

REFERENCES

1. J. Wormhoudt, Ed., Infrared Methods for Gaseous Measurements, Marcel Dekker, Inc., New York, 1985; L.A. Gross and P.R. Griffiths, "Temperature Estimation of Carbon Dioxide by Infrared Absorption Spectrometry at Medium Resolution," J. Quant. Spectrosc. Radiat. Transfer, Vol. 39, pp. 131-138, 1988; L.A. Gross and P.R. Griffiths, "Spectroscopic Temperature Estimates by Infrared Emission Spectroscopy," J. Quant. Spectrosc. Radiat. Transfer, Vol. 39, pp. 463-472, 1988; P.R. Griffiths and J.A. deHaseth, Fourier Trans. in Infrared Spectrometry, John Wiley and Sons, New York, 1986.
2. G. Herzberg, Spectra of Diatomic Molecules, Van Nostrand, New York, 1950.
3. R.J. Anderson and P.R. Griffiths, "Errors in Absorbance Measurements in Infrared Fourier Transform Spectrometry Because of Limited Instrument Resolution," Anal. Chem., Vol. 47, p. 2339, 1975.
4. R.N. Bracewell, The Fourier Transform and Its Applications, McGraw-Hill, New York, Chapter 3, 1986.
5. R.J. Anderson and P.R. Griffiths, "Determination of Rotational Temperatures of Diatomic Molecules from Absorption Spectra Measured at Moderate Resolution," J. Quant. Spectrosc. Radiat. Transfer, Vol. 17, pp. 393-401, 1977; see also Reference 3.
6. R. Herman and R.F. Wallis, "Influence of Vibration-Rotation Interaction on Line Intensities in Vibration-Rotation Bands of Diatomic Molecules," J. Chem. Phys., Vol. 23, p. 637, 1955.
7. R.S. Eng and A.W. Mantz, "Tunable Diode Laser Spectroscopy of CO₂ in the 10- to 15 μ m Spectral Region-Lineshape and Q-Branch Head Absorption Profile," J. Mol. Spec., Vol. 74, p. 331, 1979.
8. J.P. Bouanich, R. Farrenq, and C. Brobeck, "Direct Measurements of N₂ Broadened Linewidths in the CO Fundamental at Low Temperatures," Can. J. Phys., Vol. 61, p. 192, 1983; T. Nakazawa and M. Tanaka, "Measurements of Intensities and Self- and Foreign-Gas Broadened Half-Widths of Spectral Lines in the CO Fundamental Band," J. Quant. Spectrosc. Radiat. Transfer, Vol. 28, p. 409, 1982.
9. L.A. Gross, P.R. Griffiths, and J.N.-P. Sun, "Temperature Measurement by Infrared Spectrometry," in Infrared Methods for Gaseous Measurements, J. Wormhoudt, ed., Marcel Dekker, Inc., New York, p. 98, 1985.
10. K.S. Seshadri and R.N. Jones, "The Shapes and Intensities of Infrared Absorption Bands - A Review," Spectrochimica Acta, Vol. 19, p. 1013, 1963.

11. R.H. Hunt, R.A. Toth, and E.K. Plyler, "High Resolution Determination of the Widths of Self-Broadened Lines of Carbon Monoxide," J. Chem. Phys., Vol. 49, p. 3909, 1968; J.F. Bouanich and C. Brodbeck, "Mesure Des Largeurs Et Des Deplacements Des Raies De La Bande 0-2 De CO Autoperturbe Et Perturbe Par N₂, O₂, H₂, HCl, NO, Et CO₂," J. Quant. Spectrosc. Radiat. Transfer, Vol. 13, p. 1, 1973.
12. G.B. Thomas, Calculus and Analytical Geometry, Addison-Wesley, Reading, MA, 1966.
13. D.H. Rank, A.G. St. Pierre, and T.A. Wiggins, "Rotational and Vibration Constants of CO," J. Mol. Spec., Vol. 18, pp. 418-427, 1965; J.W.C. Johns, A.R.W. McKellar, and D. Weitz, "Wavelength Measurements of ¹³C¹⁶O Laser Transitions," J. Mol. Spec., Vol. 51, pp. 539-545, 1974.
14. R.J. Cvetanovic and D.L. Singleton, "Comment on the Evaluation of the Arrhenius Parameters by the Least Squares Method," Int. J. Chem. Kin., Vol. IX, p. 481, 1977.
15. G. Herzberg, Spectra of Diatomic Molecules, Van Nostrand, New York, 1950.
16. L.R. Thorne and O.I. Smith, "The Structure of Cyanogen-NO₂ Premixed Flames," Proceedings of 25th JANNAF Combustion Meeting, CPFA Publication No. 498, Vol. II, pp. 143-154, October 1988.

<u>No of Copies</u>	<u>Organization</u>
1	Office of the Secretary of Defense OUSD(A) Director, Live Fire Testing ATTN: James F. O'Bryon Washington, DC 20301-3110
2	Administrator Defense Technical Info Center ATTN: DTIC-DDA Cameron Station Alexandria, VA 22304-6145
1	HQDA (SARD-TR) WASH DC 20310-0001
1	Commander US Army Materiel Command ATTN: AMCDRA-ST 5001 Eisenhower Avenue Alexandria, VA 22333-0001
1	Commander US Army Laboratory Command ATTN: AMSI.C-DL Adelphi, MD 20783-1145
2	Commander US Army, ARDEC ATTN: SMCAR-IMI-I Picatinny Arsenal, NJ 07806-5000
2	Commander US Army, ARDEC ATTN: SMCAR-TDC Picatinny Arsenal, NJ 07806-5000
1	Director Benet Weapons Laboratory US Army, ARDEC ATTN: SMCAR-CCB-TL Watervliet, NY 12189-4050
1	Commander US Army Armament, Munitions and Chemical Command ATTN: SMCAR-ESP-L Rock Island, IL 61299-5000
1	Commander US Army Aviation Systems Command ATTN: AMSAV-DACL 4300 Goodfellow Blvd. St. Louis, MO 63120-1798

<u>No of Copies</u>	<u>Organization</u>
1	Director US Army Aviation Research and Technology Activity ATTN: SAVRT-R (Library) M/S 219-3 Ames Research Center Moffett Field, CA 94035-1000
1	Commander US Army Missile Command ATTN: AMSMI-RD-CS-R (DOC) Redstone Arsenal, AL 35898-5010
1	Commander US Army Tank-Automotive Command ATTN: AMSTA-TSL (Technical Library) Warren, MI 48397-5000
1	Director US Army TRADOC Analysis Command ATTN: ATRC-WSR White Sands Missile Range, NM 88002-5502
(Class. only) 1	Commandant US Army Infantry School ATTN: ATSH-CD (Security Mgr.) Fort Benning, GA 31905-5660
(Unclass. only) 1	Commandant US Army Infantry School ATTN: ATSH-CD-CSO-OR Fort Benning, GA 31905-5660
1	Air Force Armament Laboratory ATTN: AFATL/DLODL Eglin AFB, FL 32542-5000 <u>Aberdeen Proving Ground</u>
2	Dir, USAMSAA ATTN: AMXSY-D AMXSY-MP, H. Cohen
1	Cdr, USATECOM ATTN: AMSTE-TD
3	Cdr, CRDEC, AMCCOM ATTN: SMCCR-RSP-A SMCCR-MU SMCCR-MSI
1	Dir, VLAMO ATTN: AMSLC-VL-D

<u>No. of</u> <u>Copies</u>	<u>Organization</u>	<u>No. of</u> <u>Copies</u>	<u>Organization</u>
4	Commander US Army Research Office ATTN: R. Ghirardelli D. Mann R. Singleton R. Shaw P.O. Box 12211 Research Triangle Park, NC 27709-2211	5	Commander Naval Research Laboratory ATTN: M.C. Lin J. McDonald E. Oran J. Shnur R.J. Doyle, Code 6110 Washington, DC 20375
2	Commander US Army, ARDEC ATTN: SMCAR-AEE-B, D.S. Downs SMCAR-AEE, J.A. Lannon Picatinny Arsenal, NJ 07806-5000	1	Commanding Officer Naval Underwater Systems Center Weapons Dept. ATTN: R.S. Lazar/Code 36301 Newport, RI 02840
1	Commander US Army, ARDEC ATTN: SMCAR-AEE-BR, L. Harris Picatinny Arsenal, NJ 07806-5000	2	Commander Naval Weapons Center ATTN: T. Boggs, Code 388 T. Parr, Code 3895 China Lake, CA 93555-6001
2	Commander US Army Missile Command ATTN: AMSMI-RK, D.J. Ifshin W. Wharton Redstone Arsenal, AL 35898	1	Superintendent Naval Postgraduate School Dept. of Aeronautics ATTN: D.W. Netzer Monterey, CA 93940
1	Commander US Army Missile Command ATTN: AMSMI-RKA, A.R. Maykut Redstone Arsenal, AL 35898-5249	3	AL/LSCF ATTN: R. Corley R. Geisler J. Levine Edwards AFB, CA 93523-5000
1	Office of Naval Research Department of the Navy ATTN: R.S. Miller, Code 432 800 N. Quincy Street Arlington, VA 22217	1	AL/MKPB ATTN: B. Goshgarian Edwards AFB, CA 93523-5000
1	Commander Naval Air Systems Command ATTN: J. Ramnarace, AIR-54111C Washington, DC 20360	1	AFOSR ATTN: J.M. Tishkoff Bolling Air Force Base Washington, DC 20332
1	Commander Naval Surface Warfare Center ATTN: J.L. East, Jr., G-23 Dahlgren, VA 22448-5000	1	OSD/SDIO/UST ATTN: L. Caveny Pentagon Washington, DC 20301-7100
2	Commander Naval Surface Warfare Center ATTN: R. Bernecker, R-13 G.B. Wilmot, R-16 Silver Spring, MD 20903-5000	1	Commandant USAFAS ATTN: ATSF-TSM-CN Fort Sill, OK 73503-5600
		1	F.J. Seiler ATTN: S.A. Shackelford USAF Academy, CO 80840-6528

<u>No. of Copies</u>	<u>Organization</u>
1	University of Dayton Research Institute ATTN: D. Campbell AL/PAP Edwards AFB, CA 93523
1	NASA Langley Research Center Langley Station ATTN: G.B. Northam/MS 168 Hampton, VA 23365
4	National Bureau of Standards ATTN: J. Hastie M. Jacox T. Kashiwagi H. Semerjian US Department of Commerce Washington, DC 20234
1	Aerojet Solid Propulsion Co. ATTN: P. Micheli Sacramento, GA 95813
1	Applied Combustion Technology, Inc. ATTN: A.M. Varney P.O. Box 17885 Orlando, FL 32860
2	Applied Mechanics Reviews The American Society of Mechanical Engineers ATTN: R.E. White A.B. Wenzel 345 E. 47th Street New York, NY 10017
1	Atlantic Research Corp. ATTN: M.K. King 5390 Cherokee Avenue Alexandria, VA 22314
1	Atlantic Research Corp. ATTN: R.H.W. Waesche 7511 Wellington Road Gainesville, VA 22065
1	AVCO Everett Research Laboratory Division ATTN: D. Stickler 2385 Revere Beach Parkway Everett, MA 02149

<u>No. of Copies</u>	<u>Organization</u>
1	Battelle Memorial Institute Tactical Technology Center ATTN: J. Huggins 505 King Avenue Columbus, OH 43201
1	Cohen Professional Services ATTN: N.S. Cohen 141 Channing Street Redlands, CA 92373
1	Exxon Research & Eng. Co. ATTN: A. Dean Route 22E Annandale, NJ 08801
1	Ford Aerospace and Communications Corp. DIVAD Division Div. Hq., Irvine ATTN: D. Williams Main Street & Ford Road Newport Beach, CA 92663
1	General Applied Science Laboratories, Inc. 77 Raynor Avenue Ronkonkoma, NY 11779-6649
1	General Electric Armament & Electrical Systems ATTN: M.J. Bulman Lakeside Avenue Burlington, VT 05401
1	General Electric Ordnance Systems ATTN: J. Mandzy 100 Plastics Avenue Pittsfield, MA 01203
2	General Motors Rsch Labs Physics Department ATTN: T. Sloan R. Teets Warren, MI 48090
2	Hercules, Inc. Allegheny Ballistics Lab. ATTN: W.B. Walkup E.A. Yount P.O. Box 210 Rocket Center, WV 26726

<u>No. of Copies</u>	<u>Organization</u>
1	Honeywell, Inc. Government and Aerospace Products ATTN: D.E. Broden/ MS MN50-2000 600 2nd Street NE Hopkins, MN 55343
1	Honeywell, Inc. ATTN: R.E. Tompkins MN38-3300 10400 Yellow Circle Drive Minnetonka, MN 55343
1	IBM Corporation ATTN: A.C. Tam Research Division 5600 Cottle Road San Jose, CA 95193
1	IIT Research Institute ATTN: R.F. Remaly 10 West 35th Street Chicago, IL 60616
2	Director Lawrence Livermore National Laboratory ATTN: C. Westbrook M. Costantino P.O. Box 808 Livermore, CA 94550
1	Lockheed Missiles & Space Co. ATTN: George Lo 3251 Hanover Street Dept. 52-35/B204/2 Palo Alto, CA 94304
1	Los Alamos National Lab ATTN: B. Nichols T7, MS-B284 P.O. Box 1663 Los Alamos, NM 87545
1	National Science Foundation ATTN: A.B. Harvey Washington, DC 20550
1	Olin Ordnance ATTN: V. McDonald, Library P.O. Box 222 St. Marks, FL 32355-0222

<u>No. of Copies</u>	<u>Organization</u>
1	Paul Gough Associates, Inc. ATTN: P.S. Gough 1048 South Street Portsmouth, NH 03801-5423
2	Princeton Combustion Research Laboratories, Inc. ATTN: M. Summerfield N.A. Messina 475 US Highway One Monmouth Junction, NJ 08852
1	Hughes Aircraft Company ATTN: T.E. Ward 8433 Fallbrook Avenue Canoga Park, CA 91303
1	Rockwell International Corp. Rocketdyne Division ATTN: J.E. Flanagan/HB02 6633 Canoga Avenue Canoga Park, CA 91304
4	Sandia National Laboratories Division 8354 ATTN: R. Cattolica S. Johnston P. Mattern D. Stephenson Livermore, CA 94550
1	Science Applications, Inc. ATTN: R.B. Edelman 23146 Cumorah Crest Woodland Hills, CA 91364
3	SRI International ATTN: G. Smith D. Crosley D. Golden 333 Ravenswood Avenue Menlo Park, CA 94025
1	Stevens Institute of Tech. Davidson Laboratory ATTN: R. McAlevy, III Hoboken, NJ 07030
1	Thiokol Corporation Elkton Division ATTN: S.F. Palopoli P.O. Box 241 Elkton, MD 21921

<u>No. of</u> <u>Copies</u>	<u>Organization</u>	<u>No. of</u> <u>Copies</u>	<u>Organization</u>
1	Morton Thiokol, Inc. Huntsville Division ATTN: J. Deur Huntsville, AL 35807-7501	1	University of California, Berkeley Chemistry Department ATTN: C. Bradley Moore 211 Lewis Hall Berkeley, CA 94720
3	Thiokol Corporation Wasatch Division ATTN: S.J. Bennett P.O. Box 524 Brigham City, UT 84302	1	University of California, San Diego ATTN: F.A. Williams AMES, B010 La Jolla, CA 92093
1	United Technologies Research Center ATTN: A.C. Eckbreth East Hartford, CT 06108	2	University of California, Santa Barbara Quantum Institute ATTN: K. Schofield M. Steinberg Santa Barbara, CA 93106
3	United Technologies Corp. Chemical Systems Division ATTN: R.S. Brown T.D. Myers (2 copies) P.O. Box 49028 San Jose, CA 95161-9028	1	University of Colorado at Boulder Engineering Center ATTN: J. Daily Campus Box 427 Boulder, CO 80309-0427
1	United Aerial Propulsion Company ATTN: H.J. McSpadden Black Canyon Stage 1 Box 1140 Phoenix, AZ 85029	2	University of Southern California Dept. of Chemistry ATTN: S. Benson C. Wittig Los Angeles, CA 90007
1	Veritay Technology, Inc. ATTN: E.B. Fisher 4845 Millersport Highway P.O. Box 305 East Amherst, NY 14051-0305	1	Case Western Reserve Univ. Div. of Aerospace Sciences ATTN: J. Tien Cleveland, OH 44135
1	Brigham Young University Dept. of Chemical Engineering ATTN: M.W. Beckstead Provo, UT 84058	1	Cornell University Department of Chemistry ATTN: T.A. Cool Baker Laboratory Ithaca, NY 14853
1	California Institute of Tech. Jet Propulsion Laboratory ATTN: L. Strand/MS 512/102 4800 Oak Grove Drive Pasadena, CA 91009	1	University of Delaware ATTN: T. Brill Chemistry Department Newark, DE 19711
1	California Institute of Technology ATTN: F.E.C. Culick/ MC 301-46 204 Karman Lab. Pasadena, CA 91125	1	University of Florida Dept. of Chemistry ATTN: J. Winefordner Gainesville, FL 32611
1	University of California Los Alamos Scientific Lab. P.O. Box 1663, Mail Stop B216 Los Alamos, NM 87545		

<u>No. of Copies</u>	<u>Organization</u>	<u>No. of Copies</u>	<u>Organization</u>
3	Georgia Institute of Technology School of Aerospace Engineering ATTN: E. Price W.C. Strahle B.T. Zinn Atlanta, GA 30332	2	Princeton University Forrestal Campus Library ATTN: K. Brezinsky I. Glassman P.O. Box 710 Princeton, NJ 08540
1	University of Illinois Dept. of Mech. Eng. ATTN: H. Krier 144MEB, 1205 W. Green St. Urbana, IL 61801	1	Purdue University School of Aeronautics and Astronautics ATTN: J.R. Osborn Grissom Hall West Lafayette, IN 47906
1	Johns Hopkins University/APL Chemical Propulsion Information Agency ATTN: T.W. Christian Johns Hopkins Road Laurel, MD 20707	1	Purdue University Department of Chemistry ATTN: E. Grant West Lafayette, IN 47906
1	University of Michigan Gas Dynamics Lab Aerospace Engineering Bldg. ATTN: G.M. Faeth Ann Arbor, MI 48109-2140	2	Purdue University School of Mechanical Engineering ATTN: N.M. Laurendeau S.N.B. Murthy TSPC Chaffee Hall West Lafayette, IN 47906
1	University of Minnesota Dept. of Mechanical Engineering ATTN: E. Fletcher Minneapolis, MN 55455	1	Rensselaer Polytechnic Inst. Dept. of Chemical Engineering ATTN: A. Fontijn Troy, NY 12181
3	Pennsylvania State University Applied Research Laboratory ATTN: K.K. Kuo H. Palmer M. Micci University Park, PA 16802	1	Stanford University Dept. of Mechanical Engineering ATTN: R. Hanson Stanford, CA 94305
1	Pennsylvania State University Dept. of Mechanical Engineering ATTN: V. Yang University Park, PA 16802	1	University of Texas Dept. of Chemistry ATTN: W. Gardiner Austin, TX 78712
1	Polytechnic Institute of NY Graduate Center ATTN: S. Lederman Route 110 Farmingdale, NY 11735	1	University of Utah Dept. of Chemical Engineering ATTN: G. Flandro Salt Lake City, UT 84112
		1	Virginia Polytechnic Institute and State University ATTN: J.A. Schetz Blacksburg, VA 24061

No. of
Copies

Organization

1 Freedman Associates
 ATTN: E. Freedman
 2411 Diana Road
 Baltimore, MD 21209-1525

INTENTIONALLY LEFT BLANK.

USER EVALUATION SHEET/CHANGE OF ADDRESS

This Laboratory undertakes a continuing effort to improve the quality of the reports it publishes. Your comments/answers to the items/questions below will aid us in our efforts.

1. BRL Report Number BRL-TR-3165 Date of Report OCTOBER 1990

2. Date Report Received _____

3. Does this report satisfy a need? (Comment on purpose, related project, or other area of interest for which the report will be used.) _____

4. Specifically, how is the report being used? (Information source, design data, procedure, source of ideas, etc.) _____

5. Has the information in this report led to any quantitative savings as far as man-hours or dollars saved, operating costs avoided, or efficiencies achieved, etc? If so, please elaborate. _____

6. General Comments. What do you think should be changed to improve future reports? (Indicate changes to organization, technical content, format, etc.) _____

CURRENT
ADDRESS

Name

Organization

Address

City, State, Zip Code

7. If indicating a Change of Address or Address Correction, please provide the New or Correct Address in Block 6 above and the Old or Incorrect address below.

OLD
ADDRESS

Name

Organization

Address

City, State, Zip Code

(Remove this sheet, fold as indicated, staple or tape closed, and mail.)

-----FOLD HERE-----

DEPARTMENT OF THE ARMY

Director
U.S. Army Ballistic Research Laboratory
ATTN: SLCBR-DD-T
Aberdeen Proving Ground, MD 21061-5066
OFFICIAL BUSINESS



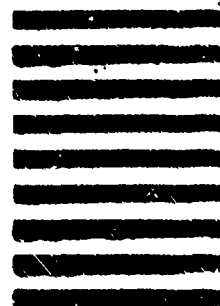
NO POSTAGE
NECESSARY
IF MAILED
IN THE
UNITED STATES

BUSINESS REPLY MAIL

FIRST CLASS PERMIT No 0001, APG, MD

POSTAGE WILL BE PAID BY ADDRESSEE

Director
U.S. Army Ballistic Research Laboratory
ATTN: SLCBR-DD-T
Aberdeen Proving Ground, MD 21005-9989



-----FOLD HERE-----